COMPUTATIONAL RESEARCH PROGRESS IN APPLIED SCIENCE & ENGINEERING (CRPASE)

CRPASE: TRANSACTIONS OF MECHANICAL ENGINEERING

Journal homepage: http://www.crpase.com

CRPASE: Transactions of Mechanical Engineering 9 (1) Article ID: 2838, 1–8, March 2023 ISSN 2423-4591

Research Article

IMU Measurement-based Bending and Deformation Identification Method for Oil and Gas Pipelines

Linjie Ma, Lin Wang *

School of Mechatronic Engineering, Southwest Petroleum University, Chengdu, 610500, China

Keywords

Oil and gas pipelines,
In-line inspection,
IMU,
Bending strain.

Abstract

Oil and gas pipelines are susceptible to local bending deformation, threatening pipeline transportation's safety. In-line inspection with inertial measurement units (IMU) is currently the main bending deformation inspection method for buried pipelines. However, the traditional bending strain calculating method based on IMU is influenced by the inherent features of the pipeline which may lead to inaccurate results and cannot truly reflect the bending deformation. To tackle this problem, a novel IMU-based bending strain calculation method is proposed to classify pipe segment, which first extracts the feature data of different pipe segments followed by classifying them into 5 types, namely hot elbow, cold elbow, weld, dent and bending deformation, and finally distinguishes bending deformation segments optimally., After analyzing the differences in bending strain values among five types of pipe features, an effective bending strain-based pipeline feature segment extraction algorithm is proposed, and classification methods are set up for different pipe features. The results show that the proposed method can effectively identify different pipe features and distinguish bending deformation segments. The recognition accuracy for elbow, weld, and dent are 99.35%, 93%, and 90.2%, respectively.

1. Introduction

The laying of long-distance oil and gas pipelines has a complex topography, and corrosion, man-made activities and long-term crustal movements can lead to a large number of bending deformations in local pipe segments, resulting in stress concentrations. In severe cases, this can even lead to leakage of transported material, causing environmental pollution and economic losses and threatening people's lives [1-4]. Currently, pipeline companies mainly use in-pipe inspection with IMU to assess bending deformation along the entire length of the pipeline [5]. The inertial sensor gyroscope reflects the attitude change of the IMU as it runs through the pipeline. The slight attitude change of the IMU as it passes through the bending deformation segments is reflected in the output of the gyroscope. The bending strain value can be calculated by attitude angle and the mileage data recorded by the mileage wheel [6-8]. In practice, the calculated bending strain value exceeding the bending strain threshold usually contains other pipe features in addition to the actual pipe bending deformation which disturbs the optimal identification of bending deformation pipe segments. Therefore the classification of pipe features which exceeds the bending strain threshold can effectively improve the accuracy of pipe bending deformation identification [9].

Currently, numerous studies about bending deformation and feature identification based on pipe centerline data from IMU have been conducted. Jaroslaw A. Czyz [10], Rui Li [11] proposed an IMU-based bending strain calculation formula for evaluating the bending deformation of pipes and verified the effectiveness of the method through

* Corresponding Author: Lin Wang
E-mail address: lincw_wang@qq.com, ORCID: https://orcid.org/0000-0003-3660-5178

Received: 10 February 2023; Revised: 19 February 2023; Accepted: 25 March 2023
https://doi.org/10.52547/crpase.9.1.2838

Academic Editor: **He Li**

Please cite this article as: L Ma, L. Wang, IMU Measurement-based Bending and Deformation Identification Method for Oil and Gas Pipelines, Computational Research Progress in Applied Science & Engineering, CRPASE: Transactions of Mechanical Engineering 9 (2022) 1–8, Article ID: 2838.

experiments. Hussein Sahli [12] discriminated elbows from straight pipes based on the change in angular velocity and judged the angle of the elbow based on the attitude angle of the sensor. Lianwu Guan[13] employed accelerometer signals to identify welds in pipe segments and Fengyuan Jiang [14] used nonlinear numerical analysis and statistical features as input to a machine learning model to achieve the identification of different deformation segments.

Existing studies focus on improving the accuracy of bending strain calculation and the identification of pipeline elbows. For the centerline measurement data of long-distance transmission pipelines with huge data size, the pipeline features that cause bending strain exceeding the threshold value are complex, and no clear method has been proposed to extract and classify the feature data quickly and accurately. To address the above problems, our study divides the analysis of pipeline IMU inspection data into two steps: feature segment signal extraction and feature classification. We propose a feature segment extraction algorithm based on the bending strain values calculated from IMU inspection data, which can effectively extract pipeline features from straight pipe data. We also design multiple identification methods for different fluctuation features of pipe types on the strain curve to distinguish bending deformation from hot elbow, cold elbow, weld, and dent. The feasibility of this method is verified using actual field measurement data.

2. Bending Strain Calculation

2.1. Curvature Calculation

The bending strain across the pipeline is mainly calculated by curvature, which is the rotation rate of the angle of the tangent direction to the arc length at a point on the curve reflecting the degree of bending at a point. The curvature k at any point on the center line of the pipe is decomposed into a horizontal curvature component kh and a vertical curvature component kv, as shown in Figure 1, where o is the center of the pipe cross-section, the x-axis is parallel to the horizontal plane where the pipe is located, the y-axis is perpendicular to the x-axis and the z-axis points in the direction of the tangent to the center line along the axial direction of the pipe.

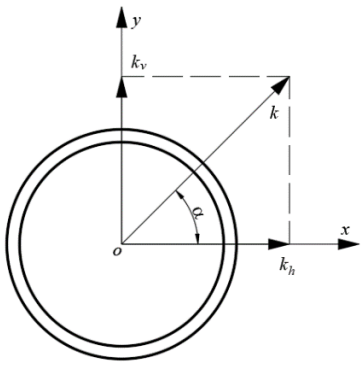

Figure 1. Decomposition of pipe curvature

The curvature at any point on the pipe is the combination of the horizontal and vertical components of curvature at that point, as shown in Eq. (1)

$$k = \sqrt{k_v^2 + k_h^2} \tag{1}$$

Supposing that the pipeline centerline r is a set of three-dimensional curve equations related to the pipeline mileage s, the expression for the three-dimensional curve r(s) is given by Eq. (2):

$$r(s) = [x(s), y(s), z(s)] \tag{2}$$

Then the tangent vector t at a point on the curve r(s) and the curvature k at that point are calculated as Eq. (3) and Eq. (4)

$$t = \frac{dr}{ds} \tag{3}$$

$$k = \frac{dt}{ds} \tag{4}$$

By projecting the centerline tangent vector t onto the local horizontal coordinate system, as shown in Figure 2, the relationship between the projection of the curvature vector k onto the coordinate system and the tangent vector t is as Eq. (5) and Eq. (6)

.

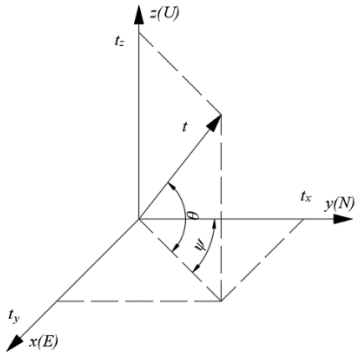

Figure 2. Projection of tangential vectors on the local horizontal coordinate system

$$\begin{cases} k_x = \frac{dt_x}{d_s} \\ k_y = \frac{dt_y}{d_s} \\ k_z = \frac{dt_z}{d_s} \end{cases} \tag{5}$$

$$|k| = \sqrt{k_x^2 + k_y^2 + k_z^2} \tag{6}$$

Assuming that the tangent vector t is a unit tangent vector, the relationship between the components of the unit tangent vector t and the pitch and heading angles is Eq. (7)

$$\begin{cases} t_x = \cos\theta \sin\psi \\ t_y = \cos\theta \cos\psi \\ t_z = \sin\theta \end{cases} \tag{7}$$

where θ and ψ are the pitch and heading angles respectively.

The expression for the relationship between the components of the curvature vector k and the attitude angle can be calculated by Eq. (3-5) as follows:

$$\begin{cases} k_x = -\sin\theta \frac{d\theta}{ds} \sin\psi + \cos\theta \cos\psi \frac{d\psi}{ds} \\ k_y = -\sin\theta \frac{d\theta}{ds} \cos\psi - \cos\theta \sin\psi \frac{d\psi}{ds} \\ k_z = \cos\theta \frac{d\theta}{ds} \end{cases} \tag{8}$$

Substituting Eq. (8) into Eq. (6) gives the total curvature value at that point (Eq. (9)).

.

$$|k| = \sqrt{k_x^2 + k_y^2 + k_z^2} = \sqrt{\left(\frac{d\theta}{ds}\right)^2 + \left(cos\,\theta\,\frac{d\psi}{ds}\right)^2} \quad (9)$$

The relationship between the total curvature and the attitude angle is obtained by Eq. (9), and in Eq. (1), the total curvature is decomposed into vertical and horizontal curvature[15]. Comparing Eq. (9) and Eq. (1), the expressions among the total curvature, the vertical and horizontal curvature components and the attitude angle can be obtained as Eq. (10)

$$\begin{cases} k_v = \frac{d\theta}{ds} \\ k_h = -cos\,\theta\,\frac{d\psi}{ds} \\ k = \sqrt{k_v^2 + k_h^2} \end{cases} \quad (10)$$

where the curvature calculation window, $d\theta$and $d\psi$, are the difference between the attitude and heading angles on the calculation window respectively.

2.2. Calculation of Bending Strain

The longitudinal "fibres" of the beam change from a straight line to a circular arc in pure bending, assuming that the cross-section remains flat and perpendicular to the deformed axial direction after bending has occurred. The two cross-sections, which are separated from each other, are rotated relative to each other around the neutral axis, as shown in Figure 3. The cross sections s1-s2 and s1'-s2' are extended to intersect at point O, which is the center of the circle of curvature of the neutral layer. Let the radius of curvature be R and the angle between the two cross-sections be $d\theta$, then the positive strain at r from the neutral layer ε is Eq. (11)

$$\varepsilon = \frac{s_2^{'} - s_1^{'}}{s_2 - s_1} = \frac{(R+r)d\theta - Rd\theta}{Rd\theta} = \frac{r}{R} \quad (11)$$

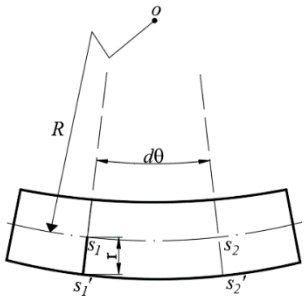

Figure 3. Beam bending deformation

Similarly, by simplifying the bending of a pipe under external forces to the pure bending of a beam, the bending strain at the outer wall of the pipe is the ratio of the radius of the pipe to the radius of curvature of the bending deformation segments. The relationship between the curvature of the pipe and the attitude angle is obtained from Eq. (12)[16]. Similarly, by dividing the bending strain into vertical and horizontal strains with the radius of curvature being the derivative of the curvature, the relationship between the bending strain and the curvature is obtained as follows:

$$\begin{cases} \varepsilon_v = \frac{D}{2} k_v \\ \varepsilon_h = \frac{D}{2} k_h \\ \varepsilon = \frac{D}{2} k \end{cases} \quad (12)$$

where D is the diameter of the pipe, $\varepsilon_v$is the vertical strain component,$\varepsilon_h$is the horizontal strain component and ε is the total bending strain.

3. Pipeline Feature Recognition

Theoretically, points where the calculated bending strain value is greater than 0.125% should be the points of concern. However, there are many actual engineering calculations where the calculated strain exceeds the reporting threshold[17], since in actual cases the calculated bending strain results are influenced by real external bending of the pipeline in addition to other characteristics of the pipeline. Any bending that occurs during the manufacture, laying and service of the pipeline is reflected in the bending strain calculation results. The pipeline is subjected to various external and internal forces that generate strains during service, but these strains cannot be completely separated from the residual plastic strains generated by processes such as hot and cold bending of the pipe. Therefore, profiling the strain calculation results and distinguishing pipe segment types that exceed the strain threshold is an important part of improving the accuracy of the bending strain assessment.

3.1. Characteristic Bending Strains of Different Pipe Types

The main types of pipe segments that can be reflected in the pipeline IMU inspection data are straight pipes, welded seams, cold bends, hot bends, bending deformations and depressions in a total of six categories. The bending strain curves for different pipe characteristics are shown in Figure 4. When the IMU travels through a straight pipe, the pipe has a smooth attitude angle and the bending strain values are small and fluctuate slightly, as shown in Figure 4(a); the bending strain at the weld is a small localized bulge, and the fluctuation magnitude of the bending strain through the weld is influenced by the residual height at the weld, as shown in Figure 4(b); when passing through an elbow, bending strain appears to change sharply over the mileage of a pipe segment. The difference between hot elbow and cold elbow is mainly reflected in the peak. Although both hot elbow and cold elbow are used to change the direction of the pipe, there is a big difference between the angles of the two. Hot elbow is constructed by heating the pipe to a certain temperature and then bending, while cold elbow is the pipe is not heated directly by external force bending. The curvature of the hot bending is greater than the cold bending which is also reflected in the bending strain results obtained from the curvature calculation and the peak bending strain of the hot elbow is greater than the cold elbow too, as shown in Figure 4 (c), 4 (d); the vertical strain at the dent is generally concave and the strain value is influenced by the degree of the dent and the length of IMU. The bending strain at the bending deformation segment is inverted "V" or continuous multiple inverted "V", and the bending strain curve

fluctuates considerably, usually more than the mileage of a pipe segment, as shown in Figure 4(f).

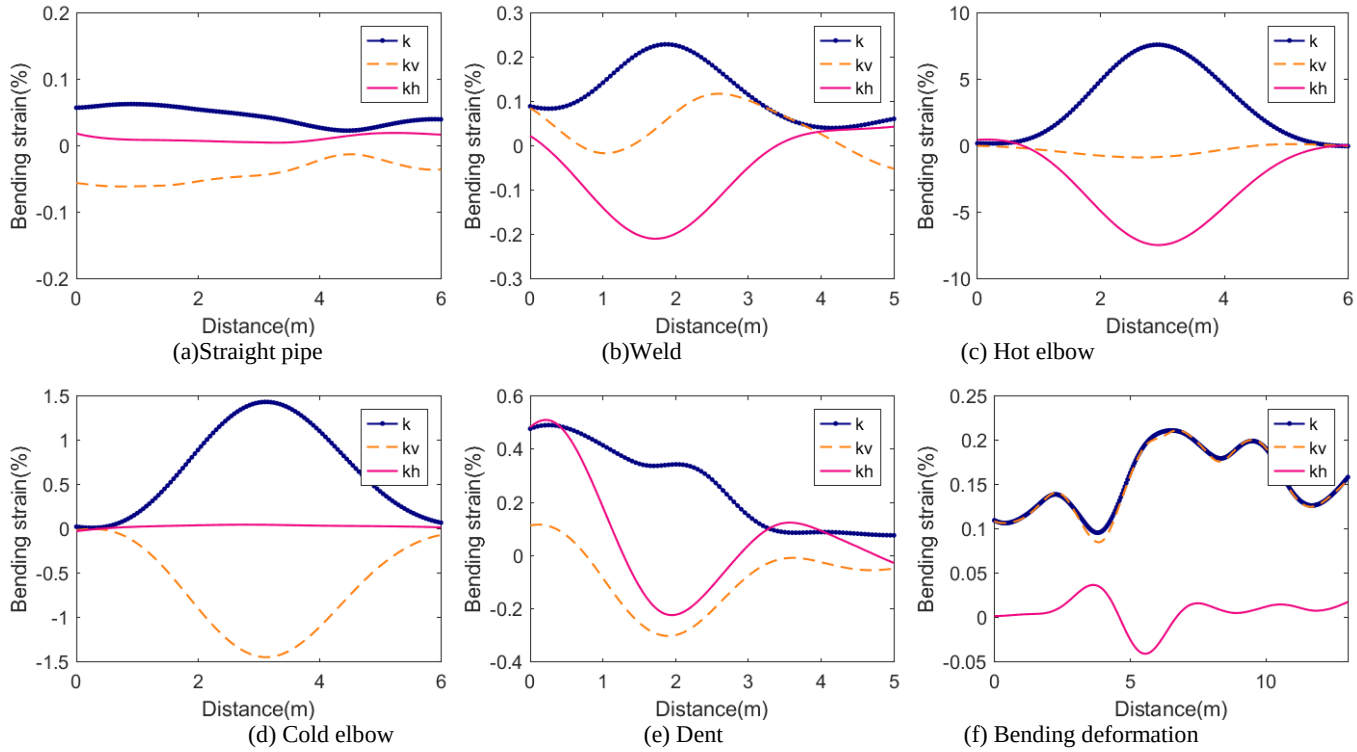

Figure 5. Differences in bending strain results for different pipe features

3.2. Feature Extraction

The characteristics of the bending strain for different pipe features are presented in section 2.1 through the alignment of the IMU inspection data. From the alignment results the bending strain of the IMU fluctuates to varying degrees as it passes through the different pipe features, and the magnitude and length of the fluctuations depend on the change in the attitude of IMU as it passes through the different pipe features. In contrast to the smooth strains in straight pipe segments, the bending strains of the IMU fluctuate to varying degrees as it passes through the pipe features, which provides the conditions for extracting the characteristic signal from the continuous bending strain curve. A method for extracting pipe features can be developed for this characteristic in the following steps.

(1) Calculate the bending strain value of the whole pipeline by using the bending strain calculation formula, select the reported threshold of bending strain, use 1/2 of the reporting threshold as the bending strain screening value, and screen all points in the whole pipeline where the bending strain is higher than the screening value as the threshold points.

(2) The minimum mileage interval is selected, and all threshold points are segmented by the minimum mileage interval. Adjacent threshold points are combined if their mileage difference is less than the minimum mileage interval and segmented if it is greater than the minimum mileage interval. The effect of this step is to divide the extracted threshold points into separate feature pipe segment data.

(3) Step 2 allows the data at some simple pipe segments to be separated. However, for some pipe segments with complex laying conditions, where multiple features are close together and a feature segment may contain more than one feature. In this case, the features cannot be effectively separated by step 2 alone. Elbows are usually laid consecutively in these kinds of pipe segments. Therefore, we perform peak inspection in these feature segments, identifying each peak point above the bending strain threshold. The peak point that reaches the elbow discrimination value is identified as an elbow, and the inflection point between two adjacent peaks is set as the split point of the adjacent elbow.

(4) Set the minimum mileage of the feature segment. Each feature segment identified in steps 2 and 3 that is less than the set minimum mileage in length is considered to be a strain threshold caused by data fluctuation errors and such feature segments will be rejected.

The above method can effectively distinguish straight pipe segments and characteristic pipe segments from continuous bending strain curves. The parameters to be set are shown in Table 1, where the reporting threshold for bending strain is generally taken to be 0.125%, the minimum mileage interval is taken to be 1D, and the bending strain at the elbow is generally between 1% and 10%. The minimum mileage of the feature segment is influenced by the length of IMU in the pipe and the length of the feature itself which can be adjusted according to the measured data.

Table 1. Parameters to be set for feature extraction

Serial number	Parameters	Main functions
1	Reporting thresholds $\varepsilon_{threshold}$	Extraction of strain points 1/2 above the threshold
2	Minimum mileage interval $s_{\min}$	Splitting and merging threshold points
3	Strain recognition values for elbows ε_{elbow}	Feature separation
4	Minimum mileage of feature segment $L_{\min}$	Error data rejection

3.3. Feature Recognition

The feature extraction method in section 2.2 promises effective separation of straight pipe data from other pipe feature data in continuous bending strain curves. In the next step, the extracted feature segments need to be differentiated by type to identify the types of pipes that cause bending strain variations.

The parameters that distinguish the different pipe features can be preset by the different trends in the bending strain curve. Among these, the significant difference between the elbow segment and the other features is mainly in the magnitude of the bending strain, while the difference between hot and cold elbow is mainly in the value of the magnitude. The mileage of the change in bending strain values caused by welds is usually short, and the amplitude of the bending strain is low. The difference in mileage between adjacent welds is within a fixed range, usually one pipe segment length apart. The dent is mainly reflected in the vertical strain, which is usually depressed, and the mileage length of the bending deformation pipe segment is generally longer than one pipe segment length. To summarize the above features, we select recognition parameters for different pipe features.

Table 2. Identification parameters for different pipe features

Serial number	Features	Identification parameters
1	Hot elbow	Bending strain amplitude
2	Cold elbow	Bending strain amplitude
3	Weld	Bending strain amplitude; mileage length; interval between adjacent characteristic segments
4	Dent	Vertical strain characteristics
5	Bending deformation	Mileage length; mean bending strain

The degree of pipe bending deformation is divided into three degrees according to the average bending strain value of the segment, namely first category (0.125%-0.2%), secondary category (0.2%-0.3%), and third category (>0.3%).

4. Example Analysis

The method is applied through the actual IMU data measured by the project. The pipeline carrying medium is natural gas which inner diameter pipeline is 1016mm. In addition to the IMU, magnetic leakage detector and geometric detector are also carried. This segment of the pipeline is approximately 200km long and the composite detector entered the collection cylinder smoothly after 20 hours of operation. The recorder was checked to be operating normally, the inspection data was clear and complete, and the pipe clearance was smooth.

Figure 6 shows the bending strain values for the 10km pipeline calculated by the bending strain formula. As can be seen from the results, the bending strain values for many segments of the pipeline exceed the threshold of 0.125% due to pipeline characteristics, thus the bending deformation of the pipeline cannot be assessed by the bending strain values alone.

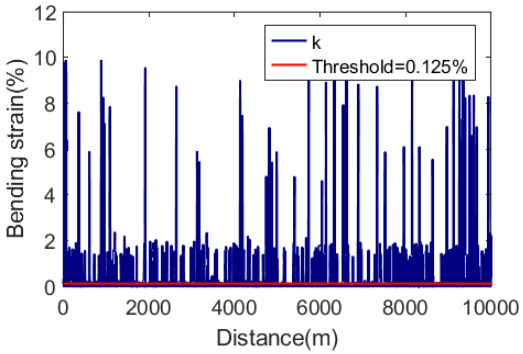

Figure 6. Bending strain values for the entire 10km pipeline

4.1.1 Feature Recognition

The first 50km of the pipeline was identified by our method with a total of 722 cold elbows and 342 hot elbows. The geometric inspection results were compared to verify the accuracy of the identification. The identification results and geometric inspection results were compared in a 5km mileage segment. From the comparison results, it is obvious that the proposed elbow identification method can effectively identify the elbows of the pipeline, and the overlap with the geometric inspection results is 99.35%.

Table 3. Comparison of elbow identification results with geometric inspection results

Mileage (km)	Cold elbow (identification)	Cold elbow (geometric inspection)	Hot elbow (identification)	Hot elbow (geometric inspection)	Contrast
1-5	78	78	21	21	/
5-10	104	102	28	28	2
10-15	34	34	23	23	/
15-20	53	53	35	35	/
20-25	92	93	57	56	2
25-30	118	116	27	27	2
30-35	46	46	55	55	/
35-40	67	68	34	34	1
40-45	48	48	29	29	/
45-50	82	82	33	33	/
Total	722	720	342	341	7 (0.65%)

Figures 7 and 8 show the distribution of 231 elbows and the radius of curvature and angle of the elbows in the first 10km of pipe respectively. The result shows that the angles of the hot and cold elbows are more diffuse in the calculation results, while the radius of curvature distribution of the hot and cold elbows is more concentrated, which is because the calculation results of the radius of curvature are influenced by the length of the pipe as well. The construction data of this pipeline segment records that the curvature is 40D for cold elbows and 10D for hot elbows, which is consistent with the calculation results.

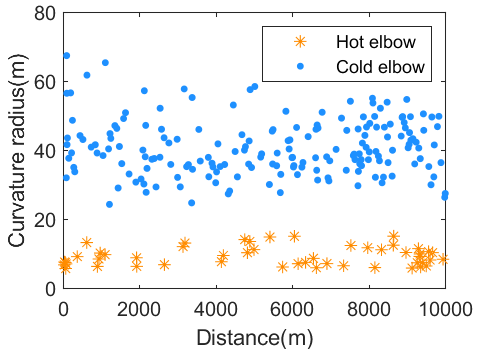

Figure 7. Radius of curvature of the elbow

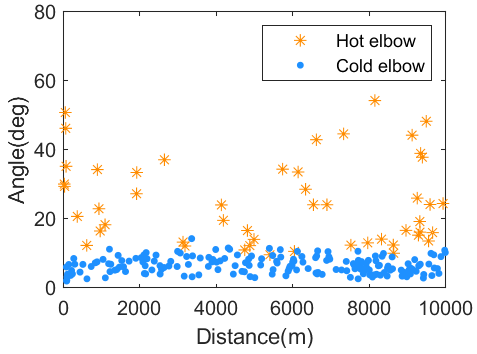

Figure 8. Angle of the elbow

4.1.2 Weld Identification

A total of 668 welds were extracted from the IMU data within the 10km pipeline using the weld identification method, and the actual number of welds in this segment was 890. In the bending strain curve, due to some welds in the pipe segment closely connecting to the elbow, the slight fluctuations caused by the welds are usually overridden by the large strain changes caused by the elbow. Therefore, the identification method does not effectively identify the weld that connects to the elbow. Excluding the welds connecting the elbows (87 x 2 = 174) there are 716 welds remaining in the 10km pipeline. Figure 9 shows the locations of the welds identified by the weld identification method. The results show that: the bending strain results caused by the welds fluctuate over a wide range, which is mostly influenced by the residual height of the welds, as mentioned earlier. The peak value of bending strain caused by the welds is much lower than the value caused by real changes in the curvature of the pipe, such as the elbow; the bending strain results caused by the welds usually fluctuate over shorter distances. In some straight, continuous pipe segments, the accuracy of weld identification by IMU is higher than in complex pipe segments with many elbows.

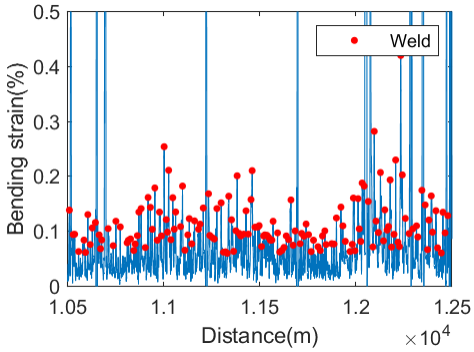

Figure 9. Location of weld in 10km local pipe segment

After excluding the welds at the elbows, the 10km pipeline was identified with an accuracy of approximately 93% by the proposed weld identification method. The error was mainly caused by the fact that the attitude does not fluctuate significantly when IMU passes through some of the welds, and therefore the peak value of bending strain induced by these welds did not reach the threshold for feature extraction.

4.1.3 Dent Identification

Dents, as external deformation defects in the pipe, are also a pipeline feature worth focusing on. As there are fewer pipe segments with dents, the results of the whole pipeline for dent identification by IMU methods and geometric deformation detection are compared (Figure 10). The results

show that the IMU bending strain-based calculations were effective in identifying pipe dents, with 61 dents detected through geometric detection and 55 identified through our identification method, with an accuracy of 90.2%.

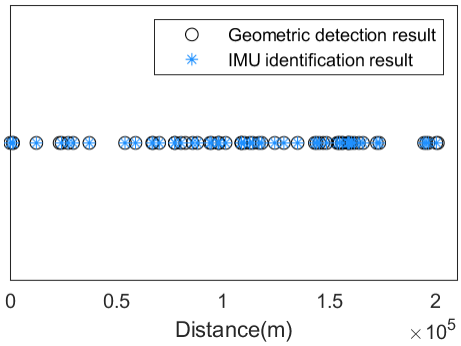

Figure. 10 Dent recognition results compared to geometric inspection results

4.2 Bending Deformation Identification

After identifying other pipe segments which cause the bending strain value to exceed the threshold such as elbows, welds, and dents through the feature identification method, the real bending deformation pipe segments are identified according to the bending deformation anomaly identification method. 74 pipe segments containing bending deformation are identified in the 200km pipeline, including 60 of the first category, 13 of the second category, and 1 of the third category. The distribution of the 74 segments over the mileage and the specific bending strain values are shown in Figure 11.

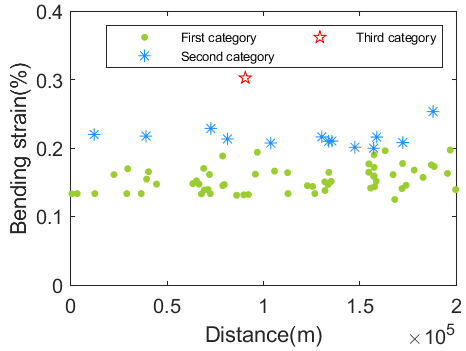

Figure 11. Mileage distribution of 74 bending deformation points and mean bending strain

5. Conclusion

The following conclusion can be drawn from this study:

(1) A bending strain calculation method based on the IMU data covering the whole pipeline is derived to reflect the bending condition of the oil and gas pipeline by the bending strain value.

(2) The differences in bending strain results when IMU passes through different pipe types are analyzed, and an extracting method for different pipe features based on bending strain results is proposed, which can effectively extract pipe features from the continuous bending strain curve.

(3) The proposed feature identification method is applied using actual engineering data, and the recognition accuracy for elbow, weld, and dent is 99.35%, 93%, and 90.2% respectively, which can effectively exclude those pipe features that cause bending strain exceeding the threshold and correctly locate the real bending deformation segment of the pipe.

6. Conflict of Interest Statement

The authors declare no conflict of interest.

Reference

[1] Feng Q, Li R, Nie B, Liu S, Zhao L, Zhang H, Literature review: Theory and application of in-line inspection technologies for oil and gas pipeline girth weld defection, Sensors 17 (2016)50.

[2] Phan HC, Duong HT, Predicting burst pressure of defected pipeline with principal component analysis and adaptive neuro fuzzy inference system, International Journal of Pressure Vessels and Piping 189 (2021)104274.

[3] Nair R, Ambati V, Detection of Leakages of Underground Pipes By GPR, LRUT, and PAUT Measurements, Computational Research Progress in Applied Science & Engineering 08 (2022).

[4] Yazdi M, A Short Communication: An Economic Assessment of Offshore Natural Gas Transferring Pipeline, Computational Research Progress in Applied Science & Engineering 07 (2021).

[5] Brockhaus S, Ginten M, Klein S, Teckert M, Stawicki O, Oevermann D, Meyer S, Storey D: In-line inspection (ILI) methods for detecting corrosion in underground pipelines. In Underground pipeline corrosion. Elsevier; 2014: 255-285

[6] Battiston A, Sharf I, Nahon M, Attitude estimation for collision recovery of a quadcopter unmanned aerial vehicle, The International Journal of Robotics Research 38 (2019)1286-1306.

[7] Chowdhury MS, Abdel-Hafez MF, Pipeline inspection gauge position estimation using inertial measurement unit, odometer, and a set of reference stations, ASCE-ASME J Risk and Uncert in Engrg Sys Part B Mech Engrg 2 (2016).

[8] Li R, Cai M, Shi Y, Feng Q, Chen P, Technologies and application of pipeline centerline and bending strain of In-line inspection based on inertial navigation, Transactions of the Institute of Measurement and Control 40 (2018)1554-1567.

[9] Morgan V, Kenny S, Power D, Gailing R: Monitoring and analysis of the effects of ground movement on pipeline integrity. In International conference on: Terrain and geohazard challenges facing onshore oil and gas pipelines: Proceedings of a three day international conference on terrain and geohazard challenges facing onshore oil and gas pipelines, organised by the Institution of Civil Engineers in association with BP Exploration and held at the Institution of Civil Engineers, London, UK, on 2–4 June 2004. Thomas Telford Publishing; 2005: 702-713.

[10] Czyz JA, Fraccaroli C, Sergeant AP, Measuring pipeline movement in geotechnically unstable areas using an inertial geometry pipeline inspection pig, (1996).

[11] Li R, Wang Z, Chen P, Development the method of pipeline bending strain measurement based on microelectromechanical systems inertial measurement unit, Science Progress 103 (2020)0036850420925231.

[12] Sahli H, El-Sheimy N, A novel method to enhance pipeline trajectory determination using pipeline junctions, Sensors 16 (2016)567.

[13] Guan L, Gao Y, Osman A, Iqbal U, Korenberg M, Noureldin A: Pipeline junction detection from accelerometer measurement using fast orthogonal search. In 2016 IEEE/ION Position, Location and Navigation Symposium (PLANS). IEEE; 2016: 21-26.

[14] Jiang F, Dong S, Collision failure risk analysis of falling object on subsea pipelines based on machine learning scheme, Engineering Failure Analysis 114 (2020)104601.
[15] Liu S, Zheng D, Dai M, Chen P, A compensation method for spiral error of pipeline bending strain in-line inspection, Journal of Testing and Evaluation 47 (2019).
[16] Zhang Q, Niu X, Shi C, Impact assessment of various IMU error sources on the relative accuracy of the GNSS/INS systems, IEEE Sensors Journal 20 (2020)5026-5038.
[17] Zhao X, Li R, Chen P, Feng W, Fu K, Zheng J, Identification and evaluation on bending deformation of China-Russia Eastern Gas Pipeline, Oil Gas Storage Transp 39 (2020)763-768.